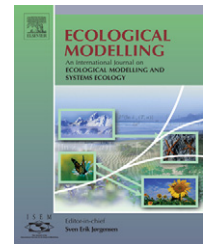


available at www.sciencedirect.comjournal homepage: www.elsevier.com/locate/ecolmodel

NEMURO—a lower trophic level model for the North Pacific marine ecosystem

Michio J. Kishi^{a,b,*}, Makoto Kashiwai^{c,h}, Daniel M. Ware^d, Bernard A. Megrey^e, David L. Eslinger^f, Francisco E. Werner^g, Maki Noguchi-Aita^b, Tomonori Azumaya^m, Masahiko Fujii^{j,w}, Shinji Hashimoto^k, Daji Huang^l, Hitoshi Iizumi^m, Yukimasa Ishida^v, Sukyung Kang^o, Gennady A. Kantakov^p, Hyun-cheol Kim^o, Kosei Komatsuⁿ, Vadim V. Navrotsky^q, S. Lan Smith^b, Kazuaki Tadokoro^{b,x}, Atsushi Tsuda^{m,r}, Orio Yamamura^m, Yasuhiro Yamanaka^{i,b}, Katsumi Yokouchi^s, Naoki Yoshie^{i,v}, Jing Zhang^t, Yury I. Zuenko^u, Vladimir I. Zvalinsky^q

^a Faculty of Fisheries Sciences, Hokkaido University N13 W8, Sapporo, Hokkaido, 060-0813 Japan

^b Ecosystem Change Research Program, Frontier Research Center for Global Change, JAMSTEC, 3173-25 Showamachi, Kanazawa-ku, Yokohama City Kanagawa 236-0001, Japan

^c Fisheries Oceanography Research Studio “OyashioYa”, Daimachi-2-6-8, Abashiri, Hokkaido, 093-0031 Japan

^d Aquatic Ecosystem Associates, 3674 Planta Road, Nanaimo, B.C. V9T 1M2, Canada

^e National Marine Fisheries Service, Alaska Fisheries Science Center, 7600 Sand Point Way NE, Bin C15700, Seattle, WA 98115-0070, USA

^f NOAA Coastal Services Center, 2234 South Hobson Ave. Charleston, SC 29405-2413, USA

^g Department of Marine Sciences, University of North Carolina, Chapel Hill, NC 27599-3300, USA

^h Department of Aquatic BioScience, Tokyo University of Agriculture, 196 Yasaka, Abashiri, Hokkaido 099-2493, Japan

ⁱ Graduate School of Environmental Science, Hokkaido University, N10W5, Kita-ku, Sapporo, Hokkaido 060-0810, Japan

^j School of Marine Sciences, 5706 Aubert Hall, University of Maine, Orono, ME 04469-5706, USA

^k National Research Institute of Far Seas Fisheries, Orido-5-7-1, Simizu-ku. Shizuoka 424-8633, Japan

^l Second Institute of Oceanography, P.O. Box 1207, Hangzhou, Zhejiang 310012, China

^m Hokkaido National Fisheries Research Institute, Katsurakoi-116, Kushiro 085-0802 Japan

ⁿ National Research Institute of Fisheries Science, Fisheries Research Agency, 2-12-4 Fukuura, Kanazawa, Yokohama, Kanagawa 236-8648, Japan

^o Korea Ocean Research & Development Institute, Ansan P.O. Box 29, Seoul 425-600, Korea

^p Sakhalin Research Institute of Fisheries and Oceanography, Komsomolskaya Street 196, Yuzhno-Sakhalinsk, PB 693016, Russia

^q Russian Pacific Oceanological Institute, Baltiyskaya Street 43, Vladivostok 690041, Russia

^r Ocean Research Institute, University of Tokyo, Minamidai 1-15-1, Nakano-ku, Tokyo 164-8639, Japan

^s Seikai National Fisheries Research Institute, 1551-8 Tairamachi, Nagasaki 851-2213, Japan

^t State Key Laboratory of Estuarine and Coastal Research, East China Normal University, 3663 North Zhongshan Road, Shanghai 200062, China

^u Pacific Fisheries Research Center, Shevchenko Alley 4 Vladivostok 690600, Russia

^v Tohoku National Fisheries Research Institute, Shinhamacho 3-27-5, Shiogama, Miyagi 985-0001, Japan

^w Sustainability Governance Project, Creative Research Initiative “Sosei”, Hokkaido University, N9W8, Kita-ku, Sapporo, Hokkaido 060-0809, Japan

^x School of Marine Science and Technology, Tokai University, Orito 3-20-1, Shimizu, Shizuoka 424-8610, Japan

* Corresponding author.

E-mail address: mjkishi@nifty.com (M.J. Kishi).

0304-3800/\$ – see front matter © 2006 Elsevier B.V. All rights reserved.

doi:10.1016/j.ecolmodel.2006.08.021

ARTICLE INFO

Article history:

Published on line 1 December 2006

Keywords:

Ecosystem model
NEMURO
North Pacific Ocean
PICES

ABSTRACT

The PICES CCCC (North Pacific Marine Science Organization, Climate Change and Carrying Capacity program) MODEL Task Team achieved a consensus on the structure of a prototype lower trophic level ecosystem model for the North Pacific Ocean, and named it the North Pacific Ecosystem Model for Understanding Regional Oceanography, “NEMURO”. Through an extensive dialog between modelers, plankton biologists and oceanographers, an extensive review was conducted to define NEMURO’s process equations and their parameter values for distinct geographic regions. We present in this paper the formulation, structure and governing equations of NEMURO as well as examples to illustrate its behavior. NEMURO has eleven state variables: nitrate, ammonium, small and large phytoplankton biomass, small, large and predatory zooplankton biomass, particulate and dissolved organic nitrogen, particulate silica, and silicic acid concentration. Several applications reported in this issue of Ecological Modelling have successfully used NEMURO, and an extension that includes fish as an additional state variable. Applications include studies of the biogeochemistry of the North Pacific, and variations of its ecosystem’s lower trophic levels and two target fish species at regional and basin-scale levels, and on time scales from seasonal to interdecadal.

© 2006 Elsevier B.V. All rights reserved.

1. Introduction

Climate change has come to the public’s attention not only for its own sake but also for its effects on the structure and function of oceanic ecosystems, and its impact on fisheries resources. It is essential to construct models that can be widely applied in the quantitative study of the world’s oceanic ecosystems. Several such attempts exist. For instance, PlankTOM5 is an ocean ecosystem and carbon cycle model that represents five plankton functional groups: the calcifiers, silicifiers, mixed phytoplankton types, and the proto- and mesozooplankton types (e.g., see Aumont et al., 2003; Le Quéré et al., 2005). PlankTOM5 is a biomass-based ecosystem model that builds on the formulations by Fasham (1993) and Fasham et al. (1993) among others. Such biomass-based ecosystem models are also referred to as a Fasham-, NPZD-, or JGOFS-type models. These are named after the Joint Global Ocean Flux Study which was a decade-long core project of the International Geosphere Biosphere Programme, IGBP, where such models were successfully used to provide estimates of carbon budgets and cycling in the oceans. Biomass or mass balance models are different from individual based or population dynamics models, which include stage- and age-structured formulations of target organisms, such as zooplankton and fish. The latter models have been developed and used in the recent GLOBEC (GLOBAL ocean ECosystem dynamics) Program, which followed JGOFS as a core ocean project of the IGBP, e.g., see discussions by Carloti et al. (2000), deYoung et al. (2004) and Runge et al. (2004).

The PICES MODEL Task Team’s approach was to use a biomass-based model as an important initial step in identifying and quantifying the relationship between climate change and ecosystem dynamics (also see Batchelder and Kashiwai, 2007). As such, a model for the northern Pacific was constructed with several compartments representing functional groups of North Pacific phytoplankton and zooplankton species, but at the same time, attempting to keep the model formulation ecologically as “simple” as possible. With this goal

in mind, the PICES MODEL Task Team held the first ‘model build-up’ workshop in Nemuro, Hokkaido, Japan in 2000, with the overall goals to: (1) select a lower trophic level model of the marine ecosystem as a consensus PICES prototype, (2) select a suite of model comparison protocols with which to examine model dynamics, (3) demonstrate the applicability of the prototype model by comparing lower trophic ecosystem dynamics among different regional study sites in the CCCC Program (see Batchelder and Kashiwai, 2007), (4) compare the prototype model with other models, (5) identify information gaps and the necessary process studies and monitoring activities to fill the gaps, and (6) discuss how to best link lower trophic level marine ecosystem models to higher trophic level marine ecosystem models, regional circulation models, and how to best incorporate these unified models into the PICES CCCC program.

The PICES CCCC prototype lower trophic level marine ecosystem model was named “NEMURO” (North Pacific Ecosystem Model for Understanding Regional Oceanography (see the Preface in this issue). NEMURO is a conceptual model representing the minimum trophic structure and biological relationships between and among all the marine ecosystem components thought to be essential in describing ecosystem dynamics in the North Pacific (Fig. 1). Boxes in Fig. 1 represent functional compartments, i.e., small phytoplankton or nitrogen concentration, and arrows represent the fluxes of nitrogen (solid arrows) and silicon (dotted arrows) between and among the state variables.

The objectives of this paper are to provide a description of the biological and physical processes contained in NEMURO, the process equations that describe the exchange of material and energy between the model state variables, the parameters used to configure the model to a location off Japan, and an example of model dynamics.

2. Model description

NEMURO consists of 11 state variables as shown schematically in Fig. 1. In the North Pacific, silicic acid ($\text{Si}(\text{OH})_4$) is

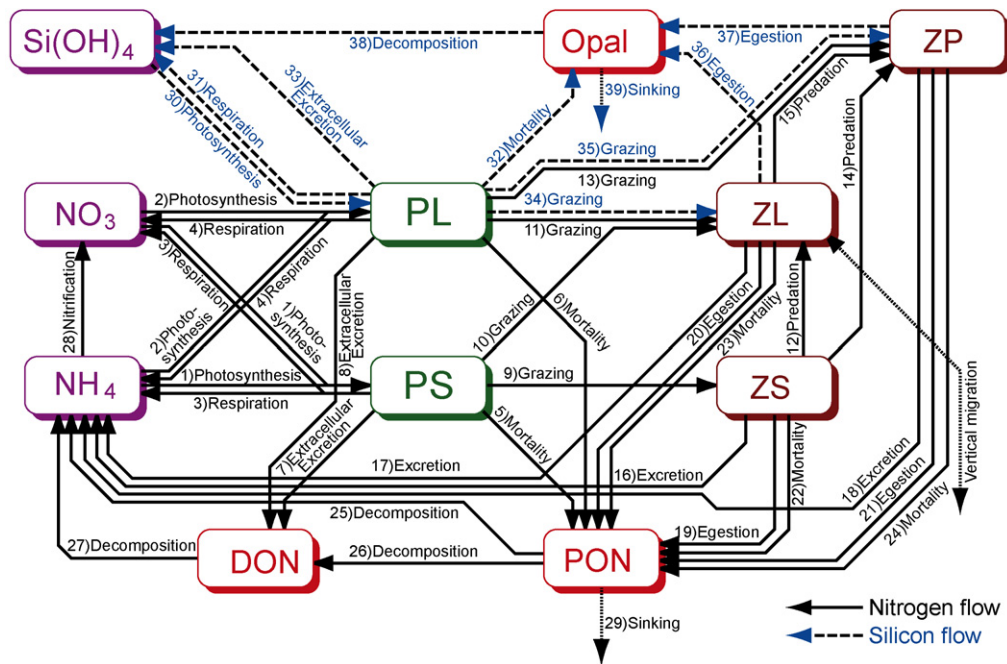


Fig. 1 – Schematic view of the NEMURO lower trophic level ecosystem model. Solid black arrows indicate nitrogen flows and dashed blue arrows indicate silicon. Dotted black arrows represent the exchange or sinking of the materials between the modeled box below the mixed layer depth.

an important limiting factor as well as nitrate (e.g., Chai et al., 2002). The subarctic Pacific is characterized by strong physical seasonality and high nitrate and low chlorophyll concentrations (HNLC). The depression of phytoplankton standing stock had previously been considered to be due to the grazing by ontogenetic migrating copepods (Parsons and Lalli, 1988). However, in situ grazing pressure appears not to be sufficient to suppress the increase of phytoplankton (Dagg, 1993; Tsuda and Sugisaki, 1994) and instead may be iron-limited. Recently, the iron hypothesis (Martin et al., 1990; Cullen, 1995) has been widely accepted in the HNLC region (e.g., Gao et al., 2003). However, we reasoned that for our purposes the effect of iron limitation can be approximated with a judicious choice of parameters (Denman and Peña, 1999) and therefore we did not include it explicitly as a separate state variable or limiting nutrient.

Mesozooplankton assemblages in the subarctic Pacific and its adjacent seas are dominated by a few species of large grazing copepods, which vertically migrate ontogenetically between the epipelagic and mesopelagic layers (Mackas and Tsuda, 1999). Several studies have suggested the trophodynamic importance of these organisms in this region (Miller et al., 1984; Miller and Clemons, 1988; Tsuda et al., 1999; Kobari et al., 2003).

Kishi et al. (2001) included ontogenetic vertical migration in their model which had as state variables: nitrate (NO_3), ammonium (NH_4), small phytoplankton biomass (PS), large phytoplankton biomass (PL), small zooplankton biomass (ZS), large zooplankton biomass (ZL), particulate organic nitrogen (PON), and dissolved organic nitrogen (DON). In the NEMURO formulation (herein), we added three additional state vari-

ables to the model of Kishi et al. (2001): predatory zooplankton biomass (ZP), particulate silica (Opal), and silicic acid concentration ($\text{Si}(\text{OH})_4$). Opal and $\text{Si}(\text{OH})_4$ are included because silicic acid is an important limiting nutrient for large phytoplankton in the North Pacific. ZP (gelatinous plankton, euphausiids or krill) is included as a predator of ZL (copepods) and ZS (ciliates). In present-day ecosystem models, the biomass of the top predator implicitly includes all other higher trophic predators and the effects of hunting by higher trophic biota in their mortality term. For an extension of NEMURO that explicitly includes fish predators on zooplankton, see Megrey et al., 2007. Thus, the biomass of the highest predator ZP is in a sense unrealistic in that it represents the total biomass of a number of species. We included ZP in NEMURO to get a more accurate representation of the biomass of ZL, which plays an important role in lower trophic ecosystems in the Northern Pacific, as well as to represent a suitable prey functional group for the higher trophic level linkages (see Megrey et al., 2007; Rose et al., 2007a).

2.1. Governing equations for nitrogen

Formulations for nitrogen fluxes between state variables are given by a set of 11 coupled ordinary differential equations. In all the formulations below, physical terms of diffusion and advection are omitted for simplicity.

$$\begin{aligned} \frac{d(\text{PS})}{dt} = & \text{Photosynthesis}(\text{PS}) - \text{respiration}(\text{PS}) - \text{mortality}(\text{PS}) \\ & - \text{extracellular excretion}(\text{PS}) - \text{grazing}(\text{PS to ZS}) \\ & - \text{grazing}(\text{PS to ZL}) \end{aligned} \quad (1)$$

$$\begin{aligned} \frac{d(PL)}{dt} = & \text{Photosynthesis (PL)} - \text{respiration (PL)} \\ & - \text{mortality (PL)} - \text{extracellular excretion (PL)} \\ & - \text{grazing (PL to ZL)} - \text{grazing(PL to ZP)} \end{aligned} \quad (2)$$

$$\begin{aligned} \frac{d(ZS)}{dt} = & \text{Grazing(PS to ZS)} - \text{predation(ZS to ZL)} \\ & - \text{predation (ZS to ZP)} - \text{mortality (ZS)} \\ & - \text{excretion (ZS)} - \text{egestion (ZS)} \end{aligned} \quad (3)$$

$$\begin{aligned} \frac{d(ZL)}{dt} = & \text{Grazing(PS to ZL)} + \text{grazing(PL to ZL)} \\ & + \text{predation(ZS to ZL)} - \text{predation (ZL to ZP)} \\ & - \text{mortality(ZL)} - \text{excretion (ZL)} - \text{egestion (ZL)} \end{aligned} \quad (4)$$

$$\begin{aligned} \frac{d(ZP)}{dt} = & \text{Grazing(PL to ZP)} + \text{predation(ZS to ZP)} \\ & + \text{predation (ZL to ZP)} - \text{mortality (ZP)} \\ & - \text{excretion(ZP)} - \text{egestion(ZP)} \end{aligned} \quad (5)$$

$$\begin{aligned} \frac{d(NO_3)}{dt} = & -(\text{Photosynthesis (PS, PL)} \\ & - \text{respiration(PS, PL)})f\text{-ratio} + \text{nitrification} \end{aligned} \quad (6)$$

$$\begin{aligned} \frac{d(NH_4)}{dt} = & -(\text{Photosynthesis(PS, PL)} \\ & - \text{respiration (PS, PL)})(1 - f\text{-ratio}) - \text{nitrification} \\ & + \text{decomposition (PON to } NH_4) \\ & + \text{decomposition (DON to } NH_4) \\ & + \text{excretion (ZS, ZL, ZP)} \end{aligned} \quad (7)$$

$$\begin{aligned} \frac{d(PON)}{dt} = & \text{Mortality(PS, PL, ZS, ZL, ZP)} + \text{egestion(ZS, ZL, ZP)} \\ & - \text{decomposition(PON to } NH_4) \\ & - \text{decomposition(PON to DON)} \end{aligned} \quad (8)$$

$$\begin{aligned} \frac{d(DON)}{dt} = & \text{Extracellular excretion (PS, PL)} \\ & + \text{decomposition (PON to DON)} \\ & - \text{decomposition (DON to } NH_4) \end{aligned} \quad (9)$$

2.2. Governing equations for silicon

$$\begin{aligned} \frac{d(Si(OH)_4)}{dt} = & -(\text{Photosynthesis (PL)} - \text{respiration (PL)}) \\ & + \text{extracellular excretion(PL)} \\ & + \text{decomposition(Opal to } Si(OH)_4) \end{aligned} \quad (10)$$

$$\begin{aligned} \frac{d(Opal)}{dt} = & \text{Mortality (PL)} + \text{egestion (ZL)} \\ & + \text{egestion(ZP)} - \text{decomposition(Opal to } Si(OH)_4) \end{aligned} \quad (11)$$

Equations describing individual processes (i.e., photosynthesis, grazing, etc.) are given in the Appendix. Parameter values were determined for two sites typifying the North Pacific (Fig. 2). Parameters values for Station A7 (41.5°N, 145.5°E) are provided in Table 1 herein. See Table 1 in Yoshie et al. (2007) for parameter values for Station Papa (50°N, 145°W).

2.3. Values of parameters

2.3.1. Parameters for temperature dependence

In this model, all biological fluxes are doubled when temperature increases by 10 °C (c.f. Kremer and Nixon, 1978). This assumption is supported by the Eppley (1972) result that photosynthetic rate is doubled when temperature increases by 10 °C. The same Q₁₀ = 2.0 relationship is applied to all other temperature-dependent rates.

2.3.2. Photosynthetic and respiratory parameters

According to Parsons et al. (1984), the range of photosynthetic rate is 0.1–16.9 mgC mgChla⁻¹ h⁻¹ (using a

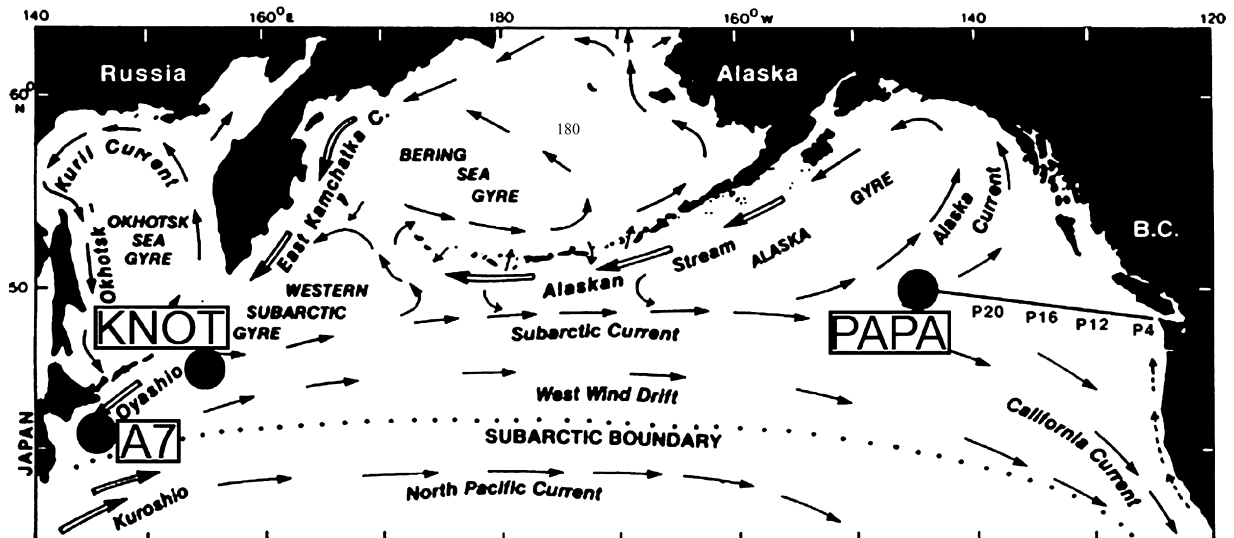


Fig. 2 – Schematic view of the North Pacific and locations of Station A7, Station Papa and Station KNOT.

Table 1 – NEMURO parameter values for Station A7

		In the text		NEMURO FORTRAN Program	
		Unit	Value	Unit	Value
Parameters for underwater light attenuation					
α_1	Light Extinction Coefficient of Sea Water	m^{-1}	0.04	m^{-1}	0.04
α_2	Self Shading Coefficient	$\mu mol N l^{-1} m^{-1}$	0.04	$mol N l^{-1} m^{-1}$	4×10^4
Parameters for small phytoplankton (PS)					
V_{maxS}	Small phytoplankton maximum photosynthetic rate	day^{-1}	0.4	sec^{-1}	$0.4 \times d2s^{-1}$
K_{NO_3S}	Small phytoplankton half saturation constant for nitrate	$\mu mol N l^{-1}$	1	$mol N l^{-1}$	1.0×10^{-6}
K_{NH_4S}	Small phytoplankton half saturation constant for ammonium	$\mu mol N l^{-1}$	0.1	$mol N l^{-1}$	0.1×10^{-6}
ψ_S	Small phytoplankton ammonium inhibition coefficient	$(\mu mol N l^{-1})^{-1}$	1.5	$(mol N l^{-1})^{-1}$	1.5×10^6
k_{GppS}	Small phytoplankton temperature coefficient for photosynthetic rate	$^{\circ}C^{-1}$	0.0693	$^{\circ}C^{-1}$	0.0693
I_{optS}	Small phytoplankton optimum light intensity	$W m^{-2}$	104.7	$ly min^{-1}$	0.15
Res_{PS0}	Small phytoplankton respiration rate at 0 °C	day^{-1}	0.03	sec^{-1}	$0.03 \times d2s^{-1}$
k_{ResPS}	Small phytoplankton temperature coefficient for respiration	$^{\circ}C^{-1}$	0.0519	$^{\circ}C^{-1}$	0.0519
γ_S	Small phytoplankton ratio of extracellular excretion to photosynthesis	No dim	0.135	No dim	0.135
Mor_{PS0}	Small phytoplankton mortality rate at 0 °C	$(\mu mol N l^{-1})^{-1} day^{-1}$	0.0585	$(mol N l^{-1})^{-1} sec^{-1}$	$5.85 \times 10^4 \times d2s^{-1}$
k_{MorPS}	Temperature coefficient for small phytoplankton mortality	$^{\circ}C^{-1}$	0.0693	$^{\circ}C^{-1}$	0.0693
Parameters for large phytoplankton (PL)					
V_{maxL}	Large phytoplankton maximum photosynthetic rate at 0 °C	day^{-1}	0.8	sec^{-1}	$0.8 \times d2s^{-1}$
K_{NO_3L}	Large phytoplankton half saturation constant for nitrate	$\mu mol N l^{-1}$	3.0	$mol N l^{-1}$	3.0×10^{-6}
K_{NH_4L}	Large Phytoplankton Half Saturation Constant for ammonium	$\mu mol N l^{-1}$	0.3	$mol N l^{-1}$	0.3×10^{-6}
K_{SiL}	Large phytoplankton half saturation constant for silicate	$\mu mol Si l^{-1}$	6.0	$mol Si l^{-1}$	6.0×10^{-6}
ψ_L	Large Phytoplankton Ammonium Inhibition Coefficient	$(\mu mol N l^{-1})^{-1}$	1.5	$(mol N l^{-1})^{-1}$	1.5×10^6
k_{GppL}	Large phytoplankton temperature coefficient for photosynthetic rate	$^{\circ}C^{-1}$	0.0693	$^{\circ}C^{-1}$	0.0693
I_{optL}	Large phytoplankton optimum light intensity	$W m^{-2}$	104.7	$ly min^{-1}$	0.15
Res_{PL0}	Large phytoplankton respiration rate at 0 °C	day^{-1}	0.03	sec^{-1}	$0.03 \times d2s^{-1}$
k_{ResPL}	Large phytoplankton temperature coefficient for respiration	$^{\circ}C^{-1}$	0.0519	$^{\circ}C^{-1}$	0.0519
γ_L	Large phytoplankton ratio of extracellular excretion to photosynthesis	No dim	0.135	No dim	0.135
Mor_{PL0}	Large phytoplankton mortality rate at 0 °C	$(\mu mol N l^{-1})^{-1} day^{-1}$	0.029	$(mol N l^{-1})^{-1} sec^{-1}$	$2.9 \times 10^4 \times d2s^{-1}$
k_{MorPL}	Temperature coefficient for large phytoplankton mortality	$^{\circ}C^{-1}$	0.0693	$^{\circ}C^{-1}$	0.0693
Parameters for small zooplankton (ZS)					
$G_{RmaxSps}$	Small zooplankton maximum grazing rate on PS at 0 °C	day^{-1}	0.4	sec^{-1}	$0.4 \times d2s^{-1}$
k_{GraS}	Small zooplankton temperature coefficient for grazing	$^{\circ}C^{-1}$	0.0693	$^{\circ}C^{-1}$	0.0693
λ_S	Small zooplankton Ivlev constant	$(\mu mol N l^{-1})^{-1}$	1.4	$(mol N l^{-1})^{-1}$	1.4×10^6
$PS2ZS^*$	Small zooplankton threshold value for grazing on Phys	$\mu mol N l^{-1}$	0.04	$mol N l^{-1}$	0.043×10^{-6}
Mor_{ZS0}	Small zooplankton mortality rate at 0 °C	$(\mu mol N l^{-1})^{-1} day^{-1}$	0.0585	$(mol N l^{-1})^{-1} sec^{-1}$	$5.85 \times 10^4 \times d2s^{-1}$
k_{MorZS}	Temperature coefficient for small zooplankton mortality	$^{\circ}C^{-1}$	0.0693	$^{\circ}C^{-1}$	0.0693
$Alpha_{ZS}$	Assimilation efficiency of small zooplankton	No dim	0.7	No dim	0.7
$Beta_{ZS}$	Growth efficiency of small zooplankton	No dim	0.3	No dim	0.3
Parameters for large zooplankton (ZL)					
GR_{maxLps}	Large zooplankton maximum grazing rate on Phys at 0 °C	day^{-1}	0.1	sec^{-1}	$0.1 \times d2s^{-1}$
GR_{maxLpl}	Large zooplankton maximum grazing rate on PhyL at 0 °C	day^{-1}	0.4	sec^{-1}	$0.4 \times d2s^{-1}$

Table 1 – (Continued)

		In the text		NEMURO FORTRAN Program	
		Unit	Value	Unit	Value
GR _{maxLzs}	Large zooplankton maximum grazing rate on ZooS at 0 °C	day ⁻¹	0.4	sec ⁻¹	0.4 × d2s ⁻¹
k _{GraL}	Large zooplankton temperature coefficient for grazing	°C ⁻¹	0.0693	°C ⁻¹	0.0693
λ _L	Large zooplankton Ivlev constant	(μmolNl ⁻¹) ⁻¹	1.4	(molNl ⁻¹) ⁻¹	1.4 × 10 ⁶
PS2ZL*	Large zooplankton threshold value for grazing on Phys	μmolNl ⁻¹	0.04	molNl ⁻¹	4.0 × 10 ⁻⁸
PL2ZL*	Large zooplankton threshold value for grazing on Phyl	μmolNl ⁻¹	0.04	molNl ⁻¹	4.0 × 10 ⁻⁸
ZS2ZL*	Large zooplankton threshold value for grazing on ZooS	μmolNl ⁻¹	0.04	molNl ⁻¹	4.0 × 10 ⁻⁸
Mor _{ZL0}	Large zooplankton mortality rate at 0 °C	(μmolNl ⁻¹) ⁻¹ day ⁻¹	0.0585	(molNl ⁻¹) ⁻¹ sec ⁻¹	5.85 × 10 ⁴ × d2s ⁻¹
k _{MorZL}	Temperature coefficient for large zooplankton mortality	°C ⁻¹	0.0693	°C ⁻¹	0.0693
Alpha _{ZL}	Assimilation efficiency of large zooplankton	No dim	0.7	No dim	0.7
Beta _{ZL}	Growth efficiency of large zooplankton	No dim	0.3	No dim	0.3
Parameters for predatory zooplankton (ZP)					
G _{RmaxPPl}	Predatory zooplankton maximum grazing rate on	day ⁻¹	0.2	sec ⁻¹	0.2 × d2s ⁻¹
G _{RmaxPZs}	Predatory zooplankton maximum grazing rate on	day ⁻¹	0.2	sec ⁻¹	0.2 × d2s ⁻¹
G _{RmaxPZl}	Predatory zooplankton maximum grazing rate on	day ⁻¹	0.2	sec ⁻¹	0.2 × d2s ⁻¹
k _{GraP}	Predatory zooplankton temperature coefficient for	°C ⁻¹	0.0693	°C ⁻¹	0.0693
λ _P	Ivlev constant of ZP	(μmolNl ⁻¹) ⁻¹	1.4	(molNl ⁻¹) ⁻¹	1.4 × 10 ⁶
PL2ZP*	Large phytoplankton threshold value for grazing by ZooP	μmolNl ⁻¹	0.04	molNl ⁻¹	0.04 × 10 ⁻⁶
ZS2ZP*	Small zooplankton threshold value for grazing by ZooP	μmolNl ⁻¹	0.04	molNl ⁻¹	0.04 × 10 ⁻⁶
ZL2ZP*	Large zooplankton threshold value for grazing by ZooP	μmolNl ⁻¹	0.04	molNl ⁻¹	0.04 × 10 ⁻⁶
ψ _{PL}	Grazing inhibition coefficient of ZooP	(μmolNl ⁻¹) ⁻¹	4.605	(molNl ⁻¹) ⁻¹	4.605 × 10 ⁶
ψ _{ZS}	Grazing inhibition coefficient of ZooP	(μmolNl ⁻¹) ⁻¹	3.01	(molNl ⁻¹) ⁻¹	3.01 × 10 ⁶
Mor _{ZP0}	Predatory zooplankton mortality rate at 0 °C	(μmolNl ⁻¹) ⁻¹ day ⁻¹	0.0585	(molNl ⁻¹) ⁻¹ sec ⁻¹	5.85 × 10 ⁴ × d2s ⁻¹
k _{MorZP}	Temperature coefficient for predatory zooplankton mortality	°C ⁻¹	0.0693	°C ⁻¹	0.0693
Alpha _{ZP}	Assimilation efficiency of predator zooplankton	No dim	0.7	No dim	0.7
Beta _{ZP}	Growth efficiency of predator zooplankton	No dim	0.3	No dim	0.3
Other parameters (decomposition, etc.)					
Nit ₀	Nitrification rate at 0 °C	day ⁻¹	0.03	sec ⁻¹	0.03 × d2s ⁻¹
k _{Nit}	Temperature coefficient for nitrification	°C ⁻¹	0.0693	°C ⁻¹	0.0693
VP2N ₀	Decomposition rate at 0 °C (PON → NH4)	day ⁻¹	0.1	sec ⁻¹	0.1 × d2s ⁻¹
k _{P2N}	Temperature coefficient for decomposition (PON → NH4)	°C ⁻¹	0.0693	°C ⁻¹	0.0693
VP2D ₀	Decomposition rate at 0 °C (PON → DON)	day ⁻¹	0.1	sec ⁻¹	0.1 × d2s ⁻¹
k _{P2D}	Temperature coefficient for decomposition (PON → DON)	°C ⁻¹	0.0693	°C ⁻¹	0.0693
VD2N ₀	Decomposition rate at 0 °C (DON → NH4)	day ⁻¹	0.02	sec ⁻¹	0.02 × d2s ⁻¹
k _{D2N}	Temperature coefficient for decomposition (DON → NH4)	°C ⁻¹	0.0693	°C ⁻¹	0.0693
VP2Si ₀	Decomposition rate at 0 °C (Opal → Si(OH)4)	day ⁻¹	0.1	sec ⁻¹	0.1 × d2s ⁻¹
k _{P2Si}	Temperature coefficient for decomposition (Opal → Si(OH)4)	°C ⁻¹	0.0693	°C ⁻¹	0.0693
RSiNPS	Si :N ratio of small phytoplankton	No dim	0	No dim	0
RSiNPL	Si:N ratio of large phytoplankton	No dim	2	No dim	2
RSiNZS	Si:N ratio of small zooplankton	No dim	0	No dim	0
RSiNZL	Si:N ratio of large zooplankton	No dim	2	No dim	2
setVP	Sinking velocity of PON	m day ⁻¹	-40	m sec ⁻¹	-40 × d2s ⁻¹
setVO	Sinking velocity of Opal	m day ⁻¹	-40	m sec ⁻¹	-40 × d2s ⁻¹

d2s = 86400 (sec day⁻¹)

Values and dimensions in the last two columns correspond to the units used in the NEMURO source code and publicly available on the <http://www.pices.int> PICES website.

typical C:Chlorophyll-a ratio of 50, which corresponds to $0.05 \text{ day}^{-1} \sim 8.1 \text{ day}^{-1}$). Many of the values for nutrient-rich waters fall in the order of $\sim 1 \text{ day}^{-1}$. In the NEMURO model, we chose 0.8 day^{-1} (for PL) and 0.4 day^{-1} (for PS) at 0°C .

For the half saturation constants, Parsons et al. (1984) found values in the range of $0.04\text{--}4.21 \mu\text{molN l}^{-1}$ for nitrate. For the eutrophic subarctic Pacific, $4.21 \mu\text{molN l}^{-1}$ and $1.30 \mu\text{molN l}^{-1}$ were reported for nitrate and ammonium, respectively (Parsons et al., 1984). In this model, the value of 3.0 (for PL) and 1.0 (for PS) $\mu\text{molN l}^{-1}$ were adopted for nitrate and 0.3 (for PL) and 0.1 (for PS) $\mu\text{molN l}^{-1}$ for ammonium. For silicic acid ($\text{Si}(\text{OH})_4$), a half saturation constant of $6.0 \mu\text{molSi l}^{-1}$ was used, which is twice that used for nitrate uptake by PL.

Optimum light intensity generally ranges between 0.03 and 0.20 ly min^{-1} (Parsons et al., 1984). A value of 0.15 ly min^{-1} (104.7 W m^{-2}) was used in our model. The ammonium inhibition coefficient ($1.5 \mu\text{molN l}^{-1}$ for PL and PS) is similar to those used by Wroblewski (1977). The respiration rate was assumed to be 0.03 day^{-1} at 0°C , comparable to values collected by Jørgensen (1979).

2.3.3. Grazing parameters

Kremer and Nixon (1978) show that maximum grazing rate values lie in the range of $0.10\text{--}2.50 \text{ day}^{-1}$. For *Calanus pacificus*, which is a relatively close species to those dominant at Station Papa (*Neocalanus plumchrus* and *Neocalanus cristatus*; Miller et al., 1984), values of $0.25, 0.22, 0.19 \text{ day}^{-1}$ were reported. Liu et al. (2005) also supports the grazing rate of $0.1\text{--}0.3 \text{ day}^{-1}$. In this model, 0.1 to 0.4 day^{-1} (at 0°C) were used.

For the Ivlev constant, Kremer and Nixon (1978) reported the range of $0.4\text{--}25.01 \text{ mgC}^{-1}$. In this model, we adopted the value of 15.01 mgC^{-1} which is close to values found for *Calanus pacificus* ($15.7, 10.0, 14.01 \text{ mgC}^{-1}$). Assuming the C:N ratio is 133:17 (Takahashi et al., 1985), this value was set to be $1.41 \mu\text{molN l}^{-1}$. For the grazing threshold value, data are scarce especially for open water species, and a value of $0.04 \mu\text{molN l}^{-1}$ ($= 4 \mu\text{gCl}^{-1}$) was assumed.

2.3.4. Nitrification rate

Data to estimate nitrification rates are few. In the North Pacific, maximum production rates of nitrate from ammonium are about 0.015 day^{-1} (Wada and Hattori, 1971). As such, the value used in this model (0.03 day^{-1} at 0°C) may be high, but preliminary experiments showed that this high value was necessary to prevent elevated ammonium concentrations compared to observed values.

2.3.5. Decomposition rate

PON decomposition rates range from 0.005 to 0.074 day^{-1} are based on a review by Matsunaga (1981). In this model, 0.1 day^{-1} (at 0°C) was used, which is close to the model value found by Matsunaga (1981).

2.3.6. Assimilation efficiency and growth efficiency

Assimilation efficiency was set to be constant although it is known to vary with food intake of zooplankton (Gaudy, 1974). A value of 70%, which corresponds to the upper limit reported for *Calanus helgolandicus* by Gaudy (1974), was assumed in this model. Sushchenya (1970) reported values for growth efficiency ranging from 4.8 to 48.9%. For this model, we assumed

30.0% for growth efficiency, roughly corresponding to the value for *Calanus helgolandicus*.

2.3.7. Mortality of phytoplankton and zooplankton

Very few quantitative data exist to approximate mortality rates of phytoplankton and zooplankton. Furthermore, data for density dependence of mortality rate, which are needed for this model, are hardly available. Thus, the values of these parameters were determined rather arbitrarily to be $0.029 (\mu\text{molN l}^{-1})^{-1} \text{ day}^{-1}$ for large phytoplankton, $0.0585 (\mu\text{molN l}^{-1})^{-1} \text{ day}^{-1}$ for zooplankton and small phytoplankton (at 0°C). Using a C:N ratio of 133:17 and a C:Chlorophyll a ratio of 50:1, phytoplankton mortality rate is 0.0045 day^{-1} at the concentration of $0.3 \mu\text{gChla l}^{-1}$, and zooplankton mortality rate is 0.015 day^{-1} at the concentration of $2.0 \mu\text{molCl}^{-1}$.

3. Implementation of NEMURO

3.1. A standard model run

The NEMURO equations and parameters described here are able to reproduce a classic North Pacific spring bloom scenario, such as one might find at Station A7 (Fig. 2). In a point implementation, such as this one, the model represents the upper, mixed layer of the ocean and the values in the model represent depth averages over that layer. There is no horizontal dimension explicitly defined in the model, but it is convenient to think of it as a 1 m^2 column of water. Yoshie et al. (2007) describe in detail the physical forcing used in this model run. The model is typically run for a number of years and, after 5 to 10 years, reaches a stable state that exhibits expected dynamics of the state variables.

A 1-year long section from a stable NEMURO run for A7 is shown in Fig. 3. In late oceanographic winter, January through March, nutrient concentrations increase to their seasonal high values due to remineralization and low uptake rates by the phytoplankton. Phytoplankton photosynthesis (and hence nutrient uptake) is low due to low-temperatures and light levels. Phytoplankton biomass (both PS and PL) slowly decreases due to respiration and grazing losses to ZS and ZP. Large zooplankton (ZL) enter the upper water column, i.e., the model domain, in late March, but the most apparent immediate effect is a small increase in the rate of ammonium production (Fig. 3). In mid-April, changes in light and temperature produce conditions suitable for phytoplankton growth, and both small and large phytoplankton begin a spring bloom period of near exponential growth. Large phytoplankton (diatoms) exhibit an earlier bloom with a biomass peak in early May. Small phytoplankton also increase, but are out-competed for nutrients by the large phytoplankton population. However, the diatom growth event is short-lived as nutrient concentrations decrease and, most importantly, as grazing losses increase due to the large zooplankton population increasing in biomass. The increased ZL grazing is shown by the decrease in PL and the increase in NH_4 , due to increased excretion by ZL, in May. After the diatom (PL) bloom is grazed down, there is a secondary bloom of flagellates (PS), and a small one of diatoms.

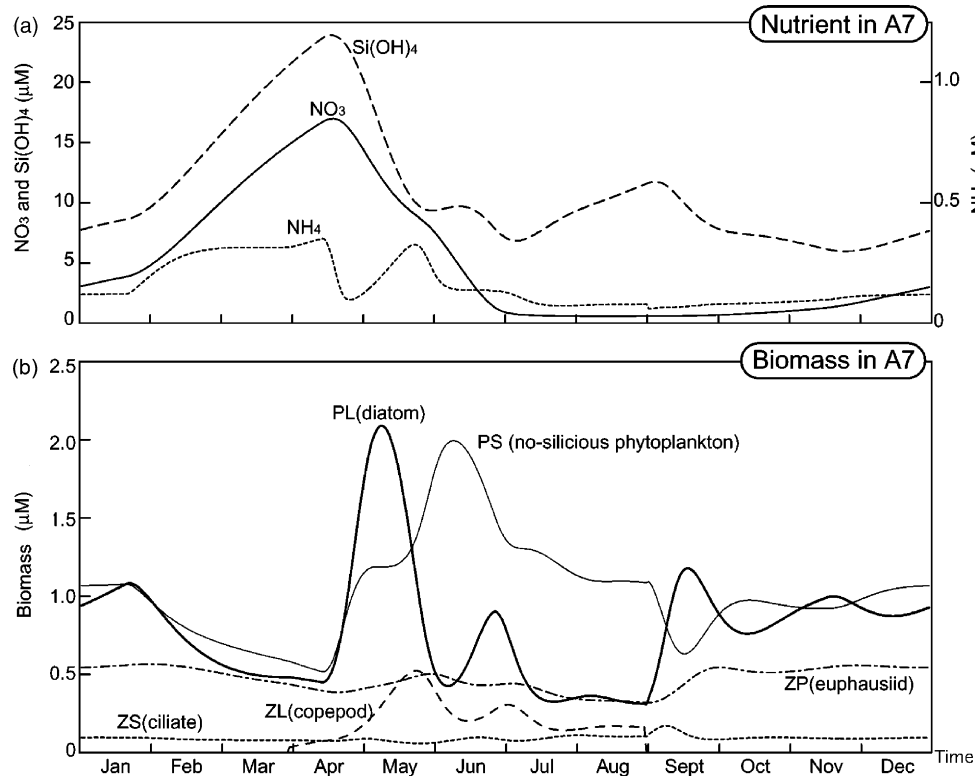


Fig. 3 – Time dependent features of all compartments of NEMURO. Daily values for the baseline simulation at station A7: (a) concentrations of nitrate (solid line), silicate (dashed line) and ammonium (dotted line), (b) biomasses of PL (thick solid line), PS (thin solid line), ZS (thin dotted line), ZL (thin dashed line), and ZP (thin dash-dotted line).

By July, the system has reached a somewhat steady state. Most of the nitrate and ammonium are gone, having been converted into the standing crops of PS, PL, ZS, SL, and ZP. Photosynthesis is sustained by the recycling of nitrogen through the ammonium pathway. Silicic acid concentrations are still above the half-saturation value, so there can be diatom (PL) production when nitrogen is available. At the end of August, large zooplankton descend from the upper water column, releasing much of the grazing pressure on PL and ZS. The small zooplankton biomass increases, leading to a small phytoplankton decrease. At the same time, the reduction in grazing from ZL allows a fall diatom bloom to occur. Another relatively stable state is reached, which lasts until the following winter, when the cycle repeats itself.

Throughout the year, biomass of small and predatory zooplankton stays relatively constant compared to that of the large zooplankton. For small zooplankton, this is because as they increase in biomass, they are quickly grazed down by both ZL and ZP. Predatory zooplankton show more variability than small zooplankton, but it is reduced relative to the large zooplankton, presumably because the additional trophic level reduces the amount of biomass that can be accumulated by ZP.

3.2. Other NEMURO applications

Several studies using NEMURO in the North Pacific already exist, e.g., Aita et al. (2003), Fujii et al. (2002), Ito et al. (2004),

Kishi et al. (2004), Kuroda and Kishi (2003), Smith et al. (2005), Yamanaka et al. (2004), and Yoshie et al. (2003). Others are reported in this issue and are reviewed by Werner et al. (2007).

Aita et al. (2003) developed a global three-dimensional physical-biological coupled model and applied it in simulations with and without ontogenetic seasonal vertical migration of large zooplankton, ZL (copepods). In the north-western Pacific, they find that primary production is higher in the case with vertical migration, that large phytoplankton (PL, diatoms) dominate, and that the presence of large zooplankton throughout the year reduces primary production by large phytoplankton (diatoms). The effect is greatest for the diatom bloom in spring. On the other hand, for regions where small phytoplankton dominate, primary production is higher in the case without vertical migration. The reason is that small zooplankton are suppressed by grazing pressure from large zooplankton, reducing grazing pressure on small phytoplankton.

Fujii et al. (2002) added a carbon cycle to NEMURO, embedded it within a vertical one-dimensional physical model and applied it to Station KNOT (Kyodo North Pacific Ocean Time series; 44°N , 155°E ; see Fig. 2). Observed seasonal cycles of ecosystem dynamics at Station KNOT, such as surface nutrient concentration and column-integrated chlorophyll-a, are successfully reproduced by the model. Sensitivity studies for several important parameters are also described.

Kuroda and Kishi (2003) applied a data assimilation technique to objectively determine NEMURO's biological parameter values. They used a Monte-Carlo method to choose eight parameters (of the over 70 parameters in NEMURO) which most impacted the simulated values of interest. Using an adjoint method, they assimilated biological and chemical data from Station A7 (see Fig. 2) into the model. Twin experiments were conducted to determine whether the data constrain those eight control variables. Model outputs using optimum parameter values determined by assimilation agreed with the data better than those obtained with parameter values obtained by a subjective first guess.

Yoshie et al. (2003) also used a one-dimensional model with NEMURO plus the addition of a carbon cycle to investigate the processes relevant to the spring diatom bloom, which play important roles in the biogeochemical cycles of the western subarctic Pacific. Their sensitivity analysis concluded that the average specific grazing rate on diatoms decreased by 35% associated with a deepening of the mixed layer, whereas the average specific photosynthesis rate of diatoms decreased by 11%. As a result, average specific net diatom growth rate during deep mixing is about 70% of its maximum during the spring diatom bloom. Deep mixing significantly affects the amplitude of the spring diatom bloom not only through increased supply of nutrients but also through dilution of zooplankton which, in turn, significantly decreases grazing pressure.

Yamanaka et al. (2004) also applied a one-dimensional model, also including NEMURO plus the addition of a carbon cycle, to Station A7 off the Hokkaido Island of Japan. The model successfully simulated the observed diatom spring bloom, large seasonal variations of nitrate and silicic acid concentrations in the surface water, and large inter-annual variations in chlorophyll-a. In Yamanaka et al. (2004), Yoshie et al. (2003) and Aita et al. (2003), the processes involving silicic acid and PL are combined into one diatom shell formation, in order to retain consistency with real ecological process observations. The equations used in NEMURO (see Appendix herein) keep the Si:N ratio constant. However, it is worth noting that the Si:N ratio may indeed vary.

Smith et al. (2005) used a one dimensional model to simulate primary production, recycling, and export of organic matter at a location near Hawaii by adding a microbial food web (MFW) to NEMURO. They compared versions of the model with and without the cycling of dissolved organic matter (DON) via the MFW, and were able to match the observed mean DOC profile near the station by tuning only the fraction of overflow DOC that is labile within their model. The simulated bulk C:N remineralization ratio from the MFW model agreed well with observed estimates for the North Pacific subtropical gyre. They concluded that overflow production and the MFW are key processes for reconciling the various biogeochemical observations and primary production measurements at this oligotrophic site.

Kishi et al. (2004) compared NEMURO with several other lower trophic level models of the northern North Pacific. The different ecosystem models are each embedded in a common three-dimensional physical model, and the simulated vertical flux of PON and the biomass of phytoplankton are compared. With proper parameter values, all of the models could reproduce primary production well, even though none

of the models explicitly included iron limitation effects. On the whole, NEMURO gave a satisfactory simulation of the vertical flux of PON in the northern North Pacific.

Ito et al. (2004) developed a fish bioenergetics model coupled to NEMURO to analyze the influence of climate changes on the growth of Pacific saury. The model was composed of three oceans domains corresponding to the Kuroshio, Oyashio, and interfrontal zone (mixed water region). In their model, biomasses of three classes of zooplankton (ZS, ZL, and ZP) were input to the bioenergetics model as prey for saury.

From the descriptions above, it is clear that NEMURO has recently become widely used for simulating the North Pacific ecosystem. Additional studies are included in this issue of Ecological Modelling.

4. Concluding remarks

The value of a model like NEMURO is that it can be applied to a wide variety of locations in the North Pacific, with only a minimal amount of tuning of the input parameters. Although the selection and determination of parameters remain an important task for future work (e.g., Kuroda and Kishi, 2003; Yoshie et al., 2007; Rose et al., 2007a), using a common set of parameters, NEMURO has been found to be useful in regional comparisons of the eastern and western North Pacific ecosystems (Werner et al., 2007).

It is important that model estimates of the production of large zooplankton be accurate because this functional group often forms the primary link to higher trophic levels (e.g., fish as added to the NEMURO model by Megrey et al., 2007 and Rose et al., 2007b). In ecosystems where autotrophic picoplankton are particularly important, the microbial food web could be better simulated by including separate picoplankton, nanophytoplankton, heterotrophic flagellates and microzooplankton groups (e.g., Le Quéré et al., 2005). However, such increase in realism comes at an expense, since it would increase the model complexity by several state variables, process equations, and rate coefficients. Incremental approaches to introducing additional complexity in NEMURO are suggested in the review by Werner et al. (2007) and references therein.

NEMURO's applications to the study of North Pacific ecosystems have yielded new insights at regional and basin scales. More importantly perhaps, NEMURO provides a framework for future studies of the variability of marine ecosystems in response to global change. Versions of the NEMURO source code are publicly available from the PICES website <http://www.pices.int>.

Acknowledgements

Authors and all participants of the NEMURO project would like to pay heartfelt thanks to the city of Nemuro, Hokkaido, Japan and their citizens for supporting our activities. Authors would like to give special thanks to Dr. R.C. Dugdale of San Francisco State University and Dr. A. Yamaguchi of Hokkaido University for providing valuable ideas relating to defining appropriate ecosystem structure and relevant parameters.

And we also thank two anonymous reviewers for improving the manuscript. We also gratefully acknowledge APN (Asia Pacific Network), the North Pacific Marine Science Organization (PICES), GLOBEC (Global Ocean Ecosystem Dynamics Program), the Heiwa-Nakajima Foundation of Japan, Japan International Science and Technology Exchange Center, City of Nemuro (Japan), and the Fisheries Research Agency (FRA) of Japan for sponsoring a series of workshops that resulted in the additional development of the NEMURO model and its applications described in papers in this issue. The participation of BAM in this research is noted as contribution FOCI-0516 to NOAA's Fisheries-Oceanography Coordinated Investigations.

Appendix A. NEMURO model equations for an 11 state variable model

Differential equations are as follows. In all the formulations below, physical terms of diffusion and advection are eliminated for simplicity.

A.1. Nitrogen (suffix *n* is added for nitrogen flow of compartments and of each process)

$$\begin{aligned} \frac{dPSn}{dt} &= GppPSn - ResPSn - MorPSn \\ &\quad - ExcPSn - GraPS2ZSn - GraPS2ZLn \\ \frac{dPLn}{dt} &= GppPLn - ResPLn - MorPLn - ExcPLn \\ &\quad - GraPL2ZLn - GraPL2ZPn \\ \frac{dZSn}{dt} &= GraPS2ZSn - GraZS2ZLn - GraZS2ZPn - MorZSn \\ &\quad - ExcZSn - EgeZSn \\ \frac{dZLn}{dt} &= GraPS2ZLn + GraPL2ZLn + GraZS2ZLn - GraZL2ZPn \\ &\quad - MorZLn - ExcZLn - EgeZLn \\ \frac{dZPn}{dt} &= GraPL2ZPn + GraZS2ZPn + GraZL2ZPn \\ &\quad - MorZPn - ExcZPn - EgeZPn \\ \frac{dNO_3}{dt} &= -(GppPSn - ResPSn)RnewS \\ &\quad - (GppPLn - ResPLn)RnewL + Nit + UPWn \\ \frac{dNH_4}{dt} &= -(GppPSn - ResPSn)(1 - RnewS) \\ &\quad - (GppPLn - ResPLn)(1 - RnewL) \\ &\quad - Nit + DecP2N + DecD2N + ExcZSn \\ &\quad + ExcZLn + ExcZPn \\ \frac{dPON}{dt} &= MorPSn + MorPLn + MorZSn + MorZLn \\ &\quad + MorZPn + EgeZSn + EgeZLn + EgeZPn \\ &\quad - DecP2N - DecP2D - SEDn \end{aligned}$$

$$\frac{dDON}{dt} = ExcPSn + ExcPLn + DecP2D - DecD2N$$

A.2. Silicon (suffix *si* is added for silicon cycle of all compartments and of each process)

$$\begin{aligned} \frac{dPLsi}{dt} &= GppPLsi - ResPLsi - MorPLsi - ExcPLi \\ &\quad - GraPL2ZLsi - GraPL2ZPsi \end{aligned}$$

$$\frac{dZLsi}{dt} = GraPL2ZLsi - EgeZLsi$$

$$\frac{dZPsi}{dt} = GraPL2ZPsi - EgeZPsi$$

$$\frac{dSi(OH)_4}{dt} = -GppPLsi + ResPLsi + ExcPLsi + UPWsi + DecP2Si$$

$$\frac{dOpal}{dt} = MorPLsi + EgeZLsi + EgeZPsi - SEDsi - DecP2Si$$

where

PSn	: Small phytoplankton biomass measured in nitrogen	($\mu\text{molN l}^{-1}$)
PLn	: Large phytoplankton biomass	($\mu\text{molN l}^{-1}$)
ZSn	: Small zooplankton biomass	($\mu\text{molN l}^{-1}$)
ZLn	: Large zooplankton biomass	($\mu\text{molN l}^{-1}$)
ZPn	: Predator zooplankton biomass	($\mu\text{molN l}^{-1}$)
NO ₃	: Nitrate concentration	($\mu\text{molN l}^{-1}$)
NH ₄	: Ammonium concentration	($\mu\text{molN l}^{-1}$)
PON	: Particulate organic nitrogen concentration	($\mu\text{molN l}^{-1}$)
DON	: Dissolved organic nitrogen concentration	($\mu\text{molN l}^{-1}$)
PLsi	: Large phytoplankton biomass measured in silicon	($\mu\text{molSi l}^{-1}$)
ZLsi	: Large zooplankton biomass	($\mu\text{molSi l}^{-1}$)
ZPsi	: Predator zooplankton biomass	($\mu\text{molSi l}^{-1}$)
Si(OH) ₄	: Silicate concentration	($\mu\text{molSi l}^{-1}$)
Opal	: Particulate Organic Silica concentration	($\mu\text{molSi l}^{-1}$)

A.3. Process equations

A.3.1. Nitrogen

- (1) GppPSn: Photosynthesis was assumed to be a function of phytoplankton concentration, temperature, nutrient concentration and intensity of light. For the dependence on nutrient concentration, Michaelis-Menten formula was adopted. Gross Primary Production rate of small phytoplankton ($\mu\text{molN l}^{-1} \text{ day}^{-1}$) consists of nutrient uptake term, temperature-dependent term, and light limitation term. Nutrient uptake term is based on Michaelis-Menten relationship and 'gourmet term of ammonium' (Wroblewski, 1977). The temperature-dependent term is

the so called “Q10” relation, whereas the light limitation term works through light inhibition of photosynthesis (Steele, 1962)

$$\begin{aligned} GppPSn = V_{\max S} & \left(\frac{NO_3}{NO_3 + K_{NO_3 S}} \exp(-\psi_S NH_4) \right. \\ & \left. + \frac{NH_4}{NH_4 + K_{NH_4 S}} \right) \exp(k_{GppS} TMP) \int_{-H}^0 \frac{I}{I_{optS}} \\ & \times \exp \left(1 - \frac{I}{I_{optS}} \right) dz PSn \end{aligned}$$

$$I = I_0 \exp(-\kappa |Z|)$$

$$\kappa = \alpha_1 + \alpha_2 (PSn + PLn)$$

where I_0 is light intensity at the sea surface, and TMP is water temperature.

RnewS: f-ratio of small phytoplankton (no dimension) which is defined by the ratio of NO_3 uptake to total uptake

$$RnewS = \frac{\frac{NO_3}{NO_3 + K_{NO_3 S}} \exp(-\psi_S NH_4)}{\frac{NO_3}{NO_3 + K_{NO_3 S}} \exp(-\psi_S NH_4) + \frac{NH_4}{NH_4 + K_{NH_4 S}}}$$

- (2) GppPLn: Gross Primary Production rate of large phytoplankton ($\mu\text{mol N l}^{-1} \text{ day}^{-1}$) which has the same formulation as PS, but contains silica and a silicate-limiting term (RSiNPL is the ratio of Si:N in PL).

$$\begin{aligned} GppPLn = V_{\max L} \min & \left\{ \frac{NO_3}{NO_3 + K_{NO_3 L}} \exp(-\psi_L NH_4) \right. \\ & \left. + \frac{NH_4}{NH_4 + K_{NH_4 L}}, \frac{Si(OH)_4}{Si(OH)_4 + K_{SiL}} / RSiNPL \right\} \\ & \times \exp(k_{GppL} TMP) \int_{-H}^0 \frac{I}{I_{optL}} \\ & \times \exp \left(1 - \frac{I}{I_{optL}} \right) dz PLn \end{aligned}$$

$$I = I_0 \exp(-\kappa |Z|)$$

$$\kappa = \alpha_1 + \alpha_2 (PSn + PLn)$$

RnewL: f-ratio of large phytoplankton (no dimension)

$$RnewL = \frac{\frac{NO_3}{NO_3 + K_{NO_3 L}} \exp(-\psi_L NH_4)}{\frac{NO_3}{NO_3 + K_{NO_3 L}} \exp(-\psi_L NH_4) + \frac{NH_4}{NH_4 + K_{NH_4 L}}}$$

- (3) ResPSn: Respiration rate of small phytoplankton ($\mu\text{mol N l}^{-1} \text{ day}^{-1}$) which is assumed to be proportional to its biomass with Q10 relation.

$$ResPSn = Res_{PS0} \exp(k_{ResPS} TMP) PSn$$

- (4) ResPLn: Respiration rate of large phytoplankton ($\mu\text{mol N l}^{-1} \text{ day}^{-1}$)

$$ResPLn = Res_{PL0} \exp(k_{ResPL} TMP) PLn$$

- (5) MorPSn: Mortality rate of small phytoplankton ($\mu\text{mol N l}^{-1} \text{ day}^{-1}$) which is assumed to be proportional to square of biomass with a Q10 relation. The reason why this term is assumed to be proportional to biomass square, is that the mortality term must be described as logistic equation.

$$MorPSn = Mor_{PS0} \exp(k_{MorPS} TMP) PSn^2$$

- (6) MorPLn: Mortality rate of large phytoplankton ($\mu\text{mol N l}^{-1} \text{ day}^{-1}$)

$$MorPLn = Mor_{PL0} \exp(k_{MorPL} TMP) PLn^2$$

- (7) ExcPSn: Extracellular excretion rate of small phytoplankton ($\mu\text{mol N l}^{-1} \text{ day}^{-1}$) which is assumed to be proportional to production.

$$ExcPSn = \gamma_S GppPSn$$

- (8) ExcPLn: Extracellular excretion rate of large phytoplankton ($\mu\text{mol N l}^{-1} \text{ day}^{-1}$)

$$ExcPLn = \gamma_L GppPLn$$

- (9) GraPS2ZSn: Grazing rate of small phytoplankton by small zooplankton ($\mu\text{mol N l}^{-1} \text{ day}^{-1}$) which is described with a temperature-dependent term (Q10) and an Ivlev equation with a feeding threshold. In this formulation, grazing rate is saturated when phytoplankton concentration is sufficiently large, while no grazing occurs when phytoplankton concentration is lower than the critical value, $PS2ZS^*$.

$$\begin{aligned} GraPS2ZSn = \text{Max}[0, GR_{\max Sps} \exp(k_{GraS} TMP) \\ \times \{ 1 - \exp(\lambda_S (PS2ZS^* - PSn)) \}] ZSn \end{aligned}$$

- (10) GraPS2ZLn: Grazing rate of small phytoplankton by large zooplankton ($\mu\text{mol N l}^{-1} \text{ day}^{-1}$)

$$\begin{aligned} GraPS2ZLn = \text{Max}[0, GR_{\max Lps} \exp(k_{GraL} TMP) \\ \times \{ 1 - \exp(\lambda_L (PS2ZL^* - ZSn)) \}] PLn \end{aligned}$$

- (11) GraPL2ZLn: Grazing rate of large phytoplankton by large zooplankton ($\mu\text{mol N l}^{-1} \text{ day}^{-1}$)

$$\begin{aligned} GraPL2ZLn = \text{Max}[0, GR_{\max Lpl} \exp(k_{GraL} TMP) \\ \times \{ 1 - \exp(\lambda_L (PL2ZL^* - PLn)) \}] ZLn \end{aligned}$$

- (12) GraZS2ZLn: Grazing rate of small zooplankton by large zooplankton ($\mu\text{mol N l}^{-1} \text{ day}^{-1}$)

$$\begin{aligned} GraZS2ZLn = \text{Max}[0, GR_{\max Lzs} \exp(k_{GraL} TMP) \\ \times \{ 1 - \exp(\lambda_L (ZS2ZL^* - ZSn)) \}] ZLn \end{aligned}$$

- (13) GraPL2ZPn: Grazing rate of large phytoplankton by predatory zooplankton ($\mu\text{mol N l}^{-1} \text{ day}^{-1}$) which includes temperature-dependent term (Q10), Ivlev relation, and ‘gourmet function’ for zooplankton.

$$\text{GraPL2ZPn} = \text{Max} \left\{ 0, \text{GR}_{\text{maxPpl}} \exp(k_{\text{GraPTMP}}) \{1 - \exp(\lambda_P(\text{PL2ZP}^* - \text{PLn}))\} \right. \\ \left. \exp(-\psi_{\text{PL}}(\text{ZLn} + \text{ZSn}))\text{ZPn} \right\}$$

- (14) GraZS2ZPn: Grazing rate of small zooplankton by predatory zooplankton ($\mu\text{molNl}^{-1} \text{day}^{-1}$)

$$\text{GraZS2ZPn} = \text{Max} \left[0, \text{GR}_{\text{maxPzs}} \exp(k_{\text{GraPTMP}}) \{1 - \exp(\lambda_P(\text{ZS2ZP}^* - \text{ZSn}))\} \right. \\ \left. \exp(-\psi_{\text{ZS}}\text{ZLn})\text{ZPn} \right]$$

- (15) GraZL2ZPn: Grazing rate of large zooplankton by predatory zooplankton ($\mu\text{molNl}^{-1} \text{day}^{-1}$)

$$\text{GraZL2ZPn} = \text{Max}[0, \text{GR}_{\text{maxPzl}} \exp(k_{\text{GraPTMP}}) \\ \times \{1 - \exp(\lambda_P(\text{ZL2ZP}^* - \text{ZLn}))\}\text{ZPn}]$$

- (16) ExcZSn: Excretion rate of small zooplankton ($\mu\text{molNl}^{-1} \text{day}^{-1}$)

- (17) ExcZLn: Excretion rate of large zooplankton ($\mu\text{molNl}^{-1} \text{day}^{-1}$)

$$\text{ExcZSn} = (\text{Alpha}_{\text{ZS}} - \text{Beta}_{\text{ZS}})\text{GraPS2ZSn}$$

$$\text{ExcZLn} = (\text{Alpha}_{\text{ZL}} - \text{Beta}_{\text{ZL}}) \\ \times (\text{GraPL2ZLn} + \text{GraZS2ZLn} + \text{GraPS2ZLn})$$

- (18) ExcZPn: Excretion rate of predatory zooplankton ($\mu\text{molNl}^{-1} \text{day}^{-1}$)

$$\text{ExcZPn} = (\text{Alpha}_{\text{ZP}} - \text{Beta}_{\text{ZP}}) \\ \times (\text{GraPL2ZPn} + \text{GraZS2ZPn} + \text{GraZL2ZPn})$$

- (19) EgeZSn: Egestion rate of small zooplankton ($\mu\text{molNl}^{-1} \text{day}^{-1}$)

$$\text{EgeZSn} = (1.0 - \text{Alpha}_{\text{ZS}})\text{GraPS2ZSn}$$

- (20) EgeZLn: Egestion rate of large zooplankton ($\mu\text{molNl}^{-1} \text{day}^{-1}$)

$$\text{EgeZLn} = (1.0 - \text{Alpha}_{\text{ZL}}) \\ \times (\text{GraPL2ZLn} + \text{GraZS2ZLn} + \text{GraPS2ZLn})$$

- (21) EgeZPn: Egestion rate of predatory zooplankton ($\mu\text{molNl}^{-1} \text{day}^{-1}$)

$$\text{EgeZPn} = (1.0 - \text{Alpha}_{\text{ZP}}) \\ \times (\text{GraPL2ZPn} + \text{GraZS2ZPn} + \text{GraZL2ZPn})$$

- (22) MorZSn: Mortality rate of small zooplankton ($\mu\text{molNl}^{-1} \text{day}^{-1}$)

$$\text{MorZSn} = \text{Mor}_{\text{ZS0}} \exp(k_{\text{MorZS}}\text{TMP})\text{ZSn}^2$$

- (23) MorZLn: Mortality rate of large zooplankton ($\mu\text{molNl}^{-1} \text{day}^{-1}$)

$$\text{MorZLn} = \text{Mor}_{\text{ZL0}} \exp(k_{\text{MorZL}}\text{TMP})\text{ZLn}^2$$

- (24) MorZPn: Mortality rate of predatory zooplankton ($\mu\text{molNl}^{-1} \text{day}^{-1}$)

$$\text{MorZPn} = \text{Mor}_{\text{ZP0}} \exp(k_{\text{MorZP}}\text{TMP})\text{ZPn}^2$$

- (25) DecP2N: Decomposition rate from PON to NH_4 ($\mu\text{molNl}^{-1} \text{day}^{-1}$) which is proportional to biomass of PON with Q10 relation to temperature.

$$\text{DecP2N} = \text{VP2N}_0 \exp(k_{\text{P2N}}\text{TMP})\text{PON}$$

- (26) DecP2D: Decomposition rate from PON to DON ($\mu\text{molNl}^{-1} \text{day}^{-1}$)

$$\text{DecP2D} = \text{VP2D}_0 \exp(k_{\text{P2D}}\text{TMP})\text{PON}$$

- (27) DecD2N: Decomposition rate from DON to NH_4 ($\mu\text{molNl}^{-1} \text{day}^{-1}$)

$$\text{DecD2N} = \text{VD2N}_0 \exp(k_{\text{D2N}}\text{TMP})\text{DON}$$

- (28) Nit: Nitrification rate ($\mu\text{molNl}^{-1} \text{day}^{-1}$) which is proportional to NH_4 with Q10 relation to temperature.

$$\text{Nit} = \text{Nit}_0 \exp(k_{\text{Nit}}\text{TMP})\text{NH}_4$$

- (29) SEDn: Sinking rate of PON ($\mu\text{molNl}^{-1} \text{day}^{-1}$)

$$\text{SEDn} = -\frac{\partial}{\partial z}(\text{setVP} \times \text{PON})$$

If upwelling exists at the bottom of the domain, we add: UPWn: Upwelling rate of NO_3 ($\mu\text{molNl}^{-1} \text{day}^{-1}$)

$$\text{UPWn} = \text{ExUP}(\text{NO}_3\text{D} - \text{NO}_3)$$

Where ExUP is upwelling velocity from the lower part of the domain, NO_3D is the NO_3 concentration at the bottom of the domain.

A.4. Silicon

- (30) GppPLsi: Gross primary production rate of large phytoplankton ($\mu\text{molSil}^{-1} \text{day}^{-1}$) which is described by multiplying Si:N ratio by the primary production term in nitrogen.

$$\text{GppPLsi} = \text{GppPLn} \times \text{RSiNPL}$$

- (31) ResPLsi: Respiration rate of large phytoplankton ($\mu\text{molSil}^{-1} \text{day}^{-1}$)

$$\text{ResPLsi} = \text{ResPLn} \times \text{RSiNPL}$$

- (32) MorPLsi: Mortality rate of large phytoplankton ($\mu\text{molSil}^{-1} \text{day}^{-1}$)

$$\text{MorPLsi} = \text{MorPLn} \times \text{RSiNPL}$$

- (33) ExcPLsi: Extracellular excretion rate of large phytoplankton ($\mu\text{molSil}^{-1} \text{day}^{-1}$)

$$\text{ExcPLsi} = \text{ExcPLn} \times \text{RSiNPL}$$

- (34) GraPL2Zlsi: Grazing rate of large phytoplankton by large zooplankton ($\mu\text{molSil}^{-1} \text{day}^{-1}$)

$$\text{GraPL2Zlsi} = \text{GraPL2ZLn} \times \text{RSiNPL}$$

- (35) GraPL2ZPsi: Grazing rate of large phytoplankton by predatory zooplankton ($\mu\text{molSi l}^{-1} \text{ day}^{-1}$)

$$\text{GraPL2ZLsi} = \text{GraPL2ZLn} \times \text{RSiNPL}$$

- (36) EgeZLsi: Egestion rate of large zooplankton ($\mu\text{molSi l}^{-1} \text{ day}^{-1}$)

$$\text{EgeZLsi} = \text{EgeZLn} \times \text{RSiNPL}$$

- (37) EgeZPsi: Egestion rate of predatory zooplankton ($\mu\text{molSi l}^{-1} \text{ day}^{-1}$)

$$\text{EgeZLsi} = \text{EgeZPn} \times \text{RSiNPL}$$

- (38) DecP2Si: Decomposition rate from Opal to Si(OH)_4 ($\mu\text{molSi l}^{-1} \text{ day}^{-1}$)

$$\text{DecP2Si} = \text{VP2Si}_0 \exp(k_{\text{P2Si}} \text{TMP}) \text{Opal}$$

- (39) SEDsi: Sedimentation rate of Opal ($\mu\text{molSi l}^{-1} \text{ day}^{-1}$)

$$\text{SEDsi} = -\frac{\partial}{\partial z} (\text{setVO} \times \text{Opal})$$

If upwelling exists at the bottom of the domain, we add:

UPWsi: Upwelling rate of Si(OH)_4 ($\mu\text{molSi l}^{-1} \text{ day}^{-1}$)

$$\text{UPWsi} = \text{ExUP}(\text{Si(OH)}_4 \text{D} - \text{Si(OH)}_4)$$

Where ExUP is upwelling velocity from the lower part of the domain, and $\text{Si(OH)}_4 \text{D}$ is the concentration of Si(OH)_4 at the bottom of the domain.

All parameter values are listed in Table 1, in the unit described above, and also in the unit used in FORTRAN program distributed widely from PICES website (<http://www.pices.int>)

REFERENCES

- Aita, M.N., Yamanaka, Y., Kishi, M.J., 2003. Effect of ontogenetic vertical migration of zooplankton on the results of NEMURO embedded in a general circulation model. *Fish. Oceanogr.* 12, 284–290.
- Aumont, O., Maier-Reimer, E., Blain, S., Monfray, P., 2003. An ecosystem model of the global ocean including Fe, SiP colimitations. *Global Biogeochem. Cycles* 17, 1060, doi:10.1029/2001GB001745.
- Batchelder, H., Kashiwai, M., 2007. Ecosystem modeling with NEMURO within the PICES climate change and carrying capacity program. *Ecol. Modell.* 202, 7–11.
- Carlotti, F., Giske, J., Werner, F.E., 2000. Modeling zooplankton dynamics. In: Harris, R.P., Wiebe, P.H., Lenz, J., Skjoldal, H.R., Huntley, M. (Eds.), *ICES Zooplankton Methodology Manual*. Academic Press, pp. 571–667.
- Chai, F., Dugdale, R.C., Peng, T.H., Wilkerson, F.P., Barber, R.T., 2002. One Dimensional Ecosystem Model of the Equatorial Pacific Upwelling System Part I: Model Development and Silicon and Nitrogen Cycle. *Deep-Sea Res. II* 49, 2713–2745.
- Cullen, J.J., 1995. Status of the iron hypothesis after the open-ocean enrichment experiment. *Limnol. Oceanogr.* 40, 1336–1343.
- Dagg, M., 1993. Sinking particles as a possible source of nutrition for the large calanoid copepod *Neocalanus cristatus* in the subarctic Pacific Ocean. *Deep-Sea Res.* 40, 1431–1445.
- Denman, K.L., Peña, M.A., 1999. A coupled 1-D biological/physical model of the northeast subarctic Pacific Ocean with iron limitation. *Deep Sea Res. II* 46, 2877–2908.
- deYoung, B., Heath, M., Werner, F.E., Chai, F., Megrey, B.A., Monfray, P., 2004. Challenges of modeling ocean basin ecosystems. *Science* 304, 1463–1466.
- Eppley, R.W., 1972. Temperature and phytoplankton growth in the sea. *Fish. Bull.* 70, 1063–1085.
- Fasham, M.J.R., 1993. Modelling the marine biota. In: Heimann, M. (Ed.), *The Global Carbon Cycle*. Springer-Verlag, Berlin, pp. 457–504.
- Fasham, M.J.R., Sarmiento, J.L., Slater, R.D., Ducklow, H.W., Williams, R., 1993. Ecosystem behaviour at Bermuda Station “S” and OWS “India”: a GCM model and observational analysis. *Global Biogeochem. Cycles* 7, 379–415.
- Fujii, M., Nojiri, Y., Yamanaka, Y., Kishi, M.J., 2002. A one-dimensional ecosystem model applied to time series Station KNOT. *Deep Sea Res. II* 49, 5441–5461.
- Gao, Y., Fan, G.Y., Sarmiento, J.L., 2003. Aeolian iron input to the ocean through precipitation scavenging: a modeling perspective and its implication for natural iron fertilization in the ocean. *J. Geophys. Res.* 108, 4221, doi:10.1029/2002JD002420.
- Gaudy, R., 1974. Feeding four species of pelagic copepods under experimental conditions. *Mar. Biol.* 25, 125–141.
- Ito, S., Kishi, M.J., Kurita, K., Oozeki, Y., Yamanaka, Y., Megrey, B.A., Werner, F.E., 2004. A fish bioenergetics model application to Pacific saury coupled with a lower trophic ecosystem model. *Fish. Oceanogr.* 13 (suppl. 1), 111–124.
- Jørgensen, S.E., 1979. *Handbook of Environmental Data and Ecological Parameters* Elsevier, p. 1162.
- Kishi, M.J., Motono, H., Kashiwai, M., Tsuda, A., 2001. An ecological-physical coupled model with ontogenetic vertical migration of zooplankton in the northwestern Pacific. *J. Oceanogr.* 57, 499–507.
- Kishi, M.J., Okunishi, T., Yamanaka, Y., 2004. A comparison of simulated particle fluxes using NEMURO and other ecosystem models in the western North Pacific. *J. Oceanogr.* 60, 63–73.
- Kobari, T., Shinada, A., Tsuda, A., 2003. Functional roles of interzonal migrating mesozooplankton in the western subarctic Pacific. *Prog. Oceanogr.* 57, 279–298.
- Kremer, J.N., Nixon, S.W., 1978. *A Coastal Marine Ecosystem: Simulation and Analysis*. Ecological Studies, vol. 24. Springer-Verlag, Heidelberg, p. 217.
- Kuroda, H., Kishi, M.J., 2003. A data assimilation technique applied to “NEMURO” for estimating parameter values. *Ecol. Modell.* 172, 69–85.
- Le Quéré, C., Harrison, S.P., Prentice, I.C., Buitenhuis, E.T., Aumont, O., Bopp, L., Claustre, H., Cotrim da Cunha, L., Geider, R., Giraud, X., Klaas, C., Kohfeld, K., Legendre, L., Manizza, M., Platt, T., Rivkin, R.B., Sathyendranath, S., Uitz, J., Watson, A.J., Wolf-Gladrow, D., 2005. Ecosystem dynamics based on plankton functional types for global ocean biogeochemistry models. *Global Change Biol.* 11, 2016–2040.
- Liu, H., Dagg, M.J., Strom, S., 2005. Grazing by calanoid copepod *Neocalanus cristatus* on the microbial food web in the coastal Gulf of Alaska. *J. Plankton Res.* 27, 647–662.
- Mackas, D., Tsuda, A., 1999. Mesozooplankton in the eastern and western subarctic Pacific: community structure, seasonal life histories, and interannual variability. *Prog. Oceanogr.* 43, 335–363.
- Martin, J.H., Gordon, R.M., Fitzwater, S.E., 1990. Iron in Antarctic waters. *Nature* 345, 156–158.
- Matsunaga, K., 1981. Studies on the decompositional processes of phytoplanktonic organic matter. *Jpn. J. Limnol.* 42, 220–229.
- Megrey, B.A., Rose, K.A., Klumb, R.A., Hay, D.E., Werner, F.E., Eslinger, D.L., Smith, S.L., 2007. A bioenergetics-based population dynamics model of Pacific herring (*Clupea harengus pallasii*) coupled to a lower trophic level

- nutrient-phytoplankton-zooplankton model: description, calibration and sensitivity analysis. *Ecol. Modell.* 202, 144–164.
- Miller, C.B., Clemons, M.J., 1988. Revised life history analysis for large grazing copepods in the subarctic Pacific Ocean. *Prog. Oceanogr.* 20, 293–313.
- Miller, C.B., Frost, B.W., Batchelder, H.P., Clemons, M.J., Conway, R.E., 1984. Life histories of large, grazing copepods in a subarctic Ocean gyre: *Neocalanus plumchrus*, *Neocalanus cristatus*, and *Eucalnus bungii* in the Northeast Pacific. *Prog. Oceanogr.* 13, 201–243.
- Parsons, T.R., Lalli, C.R., 1988. Comparative oceanic ecology of plankton communities of the subarctic Atlantic and Pacific Oceans. *Oceanogr. Mar. Biol. Annu. Rev.* 26, 317–359.
- Parsons, T.R., Takahashi, M., Hargrave, B., 1984. *Biological Oceanographic Processes*, third ed. Pergamon Press.
- Rose, K.A., Megrey, B.A., Werner, F.E., Ware, D.M., 2007a. Calibration of the NEMURO nitrogen-phytoplankton-zooplankton food web model to a coastal ecosystem: evaluation of an automated calibration approach. *Ecol. Modell.* 202, 38–51.
- Rose, K.A., Werner, F.E., Megrey, B.A., Aita, M.N., Yamanaka, Y., Hay, D., 2007b. Simulated herring growth responses in the Northeastern Pacific to historic temperature and zooplankton conditions generated by the 3-dimensional NEMURO nutrient-phytoplankton-zooplankton model. *Ecol. Modell.* 202, 184–195.
- Runge, J.A., Franks, P.J.S., Gentleman, W.C., Megrey, B.A., Rose, K.A., Werner, F.E., Zakardjian, B., 2004. Diagnosis and Prediction of Variability in Secondary Production and Fish Recruitment Processes: Developments in Physical-Biological Modelling. 13. *The Global Coastal Ocean: Multi-Scale Interdisciplinary Processes*, The Sea, pp. 413–473.
- Smith, S.L., Yamanaka, Y., Kishi, M.J., 2005. Attempting consistent simulations of Stn ALOHA with a multi-element ecosystem model. *J. Oceanogr.* 61, 1–23.
- Steele, J.H., 1962. Environmental control of photosynthesis in sea. *Limnol. Oceanogr.* 7, 137–172.
- Sushchenya, L.M., 1970. Food rations, metabolism and growth of crustaceans. In: Steele, J.H., Oliver, Boyd (Eds.), *Marine Food Chains*. Edinburgh, pp. 127–141.
- Takahashi, T., Broecker, W.S., Langer, S., 1985. Redfield ratio based on chemical data from isopycnal surfaces. *J. Geophys. Res.* 90, 6907–6924.
- Tsuda, A., Saito, H., Kasai, H., 1999. Annual variation of occurrence and growth in relation with life cycles of *Neocalanus flemingeri* and *N.plumchrus* (Calanoida Copepoda) in the western subarctic Pacific. *Mar. Biol.* 135, 533–544.
- Tsuda, A., Sugisaki, H., 1994. In-situ grazing rate of the copepod population in the western subarctic North Pacific during spring. *Mar. Biol.* 120, 203–210.
- Wada, E., Hattori, A., 1971. Nitrite metabolism in the euphotic layer of the Central North Pacific Ocean. *Limnol. Oceanogr.* 16, 766–772.
- Werner, F.E., Ito, S., Megrey, B.A., Kishi, M.J., 2007. Synthesis of the NEMURO model studies and future directions of marine ecosystem modeling. *Ecol. Modell.* 202, 211–223.
- Wroblewski, J.S., 1977. A model of phytoplankton plume formation during Oregon upwelling. *J. Mar. Res.* 35, 357–394.
- Yamanaka, Y., Yoshie, N., Fujii, M., Aita-Noguchi, M., Kishi, M.J., 2004. An ecosystem model coupled with nitrogen-silicon-carbon cycles applied to Station A-7 in the Northwestern Pacific. *J. Oceanogr.* 60, 227–241.
- Yoshie, N., Yamanaka, Y., Kishi, M.J., Saito, H., 2003. One dimensional ecosystem model simulation of effects of vertical dilution by the winter mixing on the spring diatom bloom. *J. Oceanogr.* 59, 563–572.
- Yoshie, N., Yamanaka, Y., Rose, K.A., Eslinger, D.L., Ware, D.M., Kishi, M.J., 2007. Parameter sensitivity study of the NEMURO lower trophic level marine ecosystem model. *Ecol. Modell.* 202, 26–37.